BIOCHEMISTRY
including biophysical chemistry & molecular biology
Article

Biochemistry **2010,** *49,* 9957–9963 9957
DOI: 10.1021/bi1013936

Purification of Recombinant Acyl-Coenzyme A:Cholesterol Acyltransferase 1 (ACAT1) from H293 Cells and Binding Studies between the Enzyme and Substrates Using Difference Intrinsic Fluorescence Spectroscopy[†]

Catherine C. Y. Chang,*[,‡] Akira Miyazaki,[§] Ruhong Dong,[‡] Alireza Kheirollah,[‡] Chunjiang Yu,[∥] Yong Geng,[‡] Henry N. Higgs,[‡] and Ta-Yuan Chang*[,‡]

[‡]*Department of Biochemistry, Dartmouth Medical School, Hanover, New Hampshire 03755, United States,* [§]*Department of Biochemistry, Showa University School of Medicine, Tokyo, Japan, and* [∥]*Department of Anatomy and Cell Biology, University of Illinois, Chicago, Illinois 60612, United States*

Received August 28, 2010; Revised Manuscript Received October 14, 2010

ABSTRACT: Acyl-coenzyme A:cholesterol acyltransferase 1 (ACAT1) is a membrane-bound enzyme utilizing long-chain fatty acyl-coenzyme A and cholesterol to form cholesteryl esters and coenzyme A. Previously, we had expressed tagged human ACAT1 (hACAT1) in CHO cells and purified it to homogeneity; however, only a sparse amount of purified protein could be obtained. Here we report that the hACAT1 expression level in H293 cells is 18-fold higher than that in CHO cells. We have developed a milder purification procedure to purify the enzyme to homogeneity. The abundance of the purified protein enabled us to conduct difference intrinsic fluorescence spectroscopy to study the binding between the enzyme and its substrates in CHAPS/phospholipid mixed micelles. The results show that oleoyl-CoA binds to ACAT1 with K_d = 1.9 μM and elicits significant structural changes of the protein as manifested by the significantly positive changes in its fluorescence spectrum; stearoyl-CoA elicits a similar spectrum change but much lower in magnitude. Previously, kinetic studies had shown that cholesterol is an efficient substrate and an allosteric activator of ACAT1, while its diastereomer epicholesterol is neither a substrate nor an activator. Here we show that both cholesterol and epicholesterol induce positive changes in the ACAT1 fluorescence spectrum; however, the magnitude of spectrum changes induced by cholesterol is much larger than epicholesterol. These results show that stereospecificity, governed by the 3β-OH moiety in steroid ring A, plays an important role in the binding of cholesterol to ACAT1.

Acyl-coenzyme A:cholesterol acyltransferase utilizes long-chain fatty acyl-coenzyme A and cholesterol as its substrates, producing cholesteryl esters and coenzyme A as its products. In mammals, there are two ACAT[1] genes that encode two similar but different proteins, ACAT1 (*1*) and ACAT2 (*2*−*4*). Tissue distribution studies show that ACAT1 is ubiquitously expressed, while ACAT2 is mainly expressed in intestinal enterocytes and in hepatocytes, as reviewed in ref *5*. Both ACAT1 and ACAT2 are potential drug targets for therapeutic intervention of dyslipidemia and atherosclerosis (*6*, *7*). ACAT1, ACAT2, and its close homologue diacylglycerol acyltransferase 1 (*8*) are founding members of the membrane-bound acyltransferase (MBOAT) superfamily (*9*). The MBOATs are fatty acyltransferases with multiple transmembrane domains (TMD) and with an invariant histidine (His) embedded in a long stretch of hydrophobic residues. There are more than a dozen MBOAT members that include grehlin acyltransferase (*10*, *11*) and certain lysophospholipid acyltransferases (*12* , *13*).

ACAT1 is a resident enzyme in the ER (*14*−*16*); the enzyme is homotetrameric (*17*) and contains nine TMDs, with the active site His located within TMD 7 (*18*). The recombinant human ACAT1 (hACAT1) expressed in Chinese hamster ovary (CHO) cells has been solubilized in zwitterionic detergent CHAPS and purified several thousandfold to homogeneity (*19*). With the purified enzyme, kinetic studies showed that the cholesterol substrate saturation curves, assayed either in mixed micelles or in reconstituted vesicles, were sigmoidal, while the oleoyl-coenzyme A substrate saturation curve was hyperbolic, suggesting that ACAT1 is an allosteric enzyme activated by its own substrate cholesterol (*19*). Upon activation by cholesterol, the enzyme becomes promiscuous and is able to accommodate a variety of sterols with 3β-OH at ring A as its substrates (*20*, *21*). A major drawback of the CHO cell expression system for purifying ACAT1 is that only a low quantity of ACAT1 protein could be obtained (*19*). The sparse amount of purified protein available has hampered the research progress of ACAT1 structure−function analysis. We have sought to increase hACAT1 yield by using various other expression systems that include *Escherichia coli*, yeast, and the baculovirus-infected insect cells but were unsuccessful. In the current work, we report that hACAT1 can be expressed in H293 cells at levels much higher than that in the CHO cells. We next developed an efficient purification procedure to purify the recombinant hACAT1 from H293 cells to homogeneity. The improved expression and purification procedure enabled us to obtain enough purified protein to demonstrate that hACAT1 is a highly fluorescent protein. We have exploited this feature by performing binding studies between hACAT1 and its substrates.

[†]This work is supported by NIH Grant RO1 HL60306 to T.-Y.C. and C.C.Y.C. and NIH Grant RO1 GM069818 to H.N.H.

*Corresponding authors. Phone: (603) 650-1809. Fax: (603) 650-1129. E-mail: catherine.chang@dartmouth.edu; ta.yuan.chang@dartmouth.edu.

[1]Abbreviations: ACAT, acyl-coenzyme A:cholesterol acyltransferase; CHO, Chinese hamster ovary; CoA, coenzyme A; CHAPS, 3-[(3-cholamidopropyl)dimethylammonio]-1-propanesulfonate; PC, phosphatidylcholine; TMD, transmembrane domain. His, histidine; KCl, potassium chloride.

Published on Web 10/22/2010

EXPERIMENTAL PROCEDURES

Materials. The rabbit polyclonal antibodies (DM10, DM102) against the N-terminal fragment (1−131) of human ACAT1 were described previously (*14*). Anti-FLAG M2 antibody, anti-FLAG M2 affinity gel, the 3× Flag peptide, CHAPS, taurocholate, oleoyl-CoA, stearoyl-CoA, egg PC, cholesteryl oleate, cholesterol, fatty acid-free bovine serum albumin, and protease inhibitor cocktails were all from Sigma. Ni-NTA His-Bind resin came from Novagen. Fugene 6 was from Roche. The software program PRISM 5 was from GraphPad. [^{3}H]Cholesterol came from Perkin-Elmer. [^{3}H]Oleoyl-coenzyme A was synthesized as described (*22*).

Cell Culture. The HEK293S cell line was kindly provided by Dr. Philip Reeves (*23*). Cells were grown as monolayers in DMEM supplemented with 10% new born serum (NBS) at 37 °C in a 5% CO_2 incubator.

Construction of Plasmid HisACAT1/Flag and Its Expression in H293 Cells. To aid in enzyme purification, a Flag octapeptide (DYKDDDDK, 1012 Da) was inserted at the C-terminus of HisACAT1 cDNA (*18*), which contains a fragment of 6-histidine (His) tag, and the enterokinase cleavage recognition sequence (35 amino acids and 4057 Da) was inserted at the N-terminus of human ACAT1 (*19*). This fragment (HisACAT1/Flag) was then ligated into the mammalian expression vector pAG3-Zeo (*24*), using the *Bam*HI and *Apa*I cloning sites. This plasmid was transfected into HEK293S; individual stable clones were isolated by selecting cells resistant to zeocin at 400 μg/mL.

Purification of the HisACAT1/Flag Protein. HEK293S stably expressing HisACAT1/Flag were seeded in 55 of 145 mm dishes for 2−3 days until the cells reached at confluency. Cells were rinsed 2× with PBS and harvested by directly solublilizing the cells with buffer A (1 M KCl, 2.5% CHAPS in 50 mM KH_2PO_4 buffer at pH 7.8; 1 mL/dish). The detergent-solubilized cell extracts were subjected to 100000*g* spin for 1 h at 4 °C; the solubilized enzyme preparation was loaded onto a 20 mL size His-Bind resin. The column was washed by using 4 column volumes of 20 mM imidazole in buffer B (0.5 M KCl, 0.5% CHAPS in 50 mM KH_2PO_4 buffer at pH 7.8). The fusion protein was eluted off the column by using 2 column volumes of 500 mM imidazole in buffer B. The eluate was then applied to a 5 mL FLAG M2 affinity gel and allowed to flow by gravity. After extensive buffer washes using buffer B, the HisACAT1/Flag fusion protein was eluted off the column by 3 column volumes of 100 μg/mL FLAG peptide in buffer B. The purified fusion protein could be stored at −80 °C for at least 6 months without detectable loss in enzyme activity.

ACAT Enzyme Assay. To monitor enzyme activity during enzyme purification, the enzyme solubilized in the detergent CHAPS was assayed in preformed taurocholate/cholesterol/phosphatidylcholine (PC) mixed micelles as described previously (*25*), with a final concentration of taurocholate at 9.3 mM, PC at 11.2 mM, and cholesterol at 1.6 mM. The amount of mixed micelle solution was used to dilute the detergent presented in the enzyme preparation, so the final CHAPS/PC molar ratio was less than 0.4. The fatty acyl-CoA substrate saturation curves and cholesterol substrate saturation curves were performed under the same conditions as described previously (*25*).

Intrinsic Fluorescence Measurement. Fluorescence measurements were generated by using an ISS PC1 photocounting fluorescence spectrophotometer (model 90095). This instrument has continuously reproducible slits ranging from 0.4 to 32 nm band-pass. The excitation slit width was set at 2 nm. The wavelength for excitation was set at 295 nm in order to minimize the contribution of tyrosine residues to the fluorescence. Purified HisACAT1/Flag was concentrated by using 30K Amicon centrifugal filters such that the final concentration of the protein was 100−200 ng/μL (1.5−3 μM) and stored at −80 °C until usage. Unless stated otherwise, the fluorescence measurements were performed at pH 7.8 with 50 mM potassium phosphate, 0.5 M KCl, and 8.13 mM CHAPS. Sterol (cholesterol, epicholesterol, coprostanol, and epicoprostanol) was prepared as CHAPS/PC/sterol mixed micelles (with CHAPS at 8.13 mM, PC at 4 mM, and with varying concentrations of sterols as indicated) and stored at 20 °C in the dark until usage. The fatty acyl-CoAs were dissolved in 20 mM sodium acetate at pH 6.4 as a 2 mM stock and stored at −80 °C until usage. Before the experiment started, all reagents were kept on ice in the dark. To begin the experiment, 50 μL of mixed micelles without or with sterols was added into a Hellma microcuvette (Type 105.251-QS) with 3 mm light path. Twenty-five microliters of ACAT1 protein (in 8.13 mM CHAPS and 0.5 M KCl) was then added and rapidly mixed. Fluorescence was monitored within 15 s of adding the enzyme. The sample compartment of the instrument was maintained at 20 °C. The fluorescence emission spectrum was scanned in 2 min between 310 and 410 nm. The differences in fluorescence intensity at 10 intervals within 325−335 nm were averaged in order to calculate the ΔF value between the ligated protein vs that of the unligated protein.

Gel Electrophoresis and Staining. Samples were run on 8% SDS−PAGE as described previously (*25*). The gels were stained with the SilverQuest silver staining kit from Invitrogen.

RESULTS

Expression and Purification of Recombinant hACAT1 (HisACAT1/Flag) in H293 Cells. We transfected the H293 cells with the mammalian expression vector pAG3 that contained the hACAT1 tagged with 6His at the N-terminus and Flag at the C-terminus (designated as HisACAT1/Flag) as the insert. Various clones that stably express the recombinant protein were then isolated (see Experimental Procedures). Western blotting was used to monitor the hACAT1 protein expression level. The results show that the tagged hACAT1, with an apparent molecular mass of 56 kDa in SDS−PAGE, can be amply expressed in H293 cells (Figure 1A, rightmost two lanes). The expression level of the HisACAT1/Flag shown in Figure 1A is representative of several stable clones independently isolated from H293 cells. H293 cell is a human cell line and expresses (untagged) hACAT1 endogenously (Figure 1A, the fifth and sixth lanes from the left), with an apparent molecular mass of 50 kDa. The endogenous hACAT1 could also be detected in the H293 cells that stably express HisACAT1/FLAG, especially when a larger amount of cellular protein (50 μg) was employed in the Western analysis (Figure 1A, last lane from the left). Other results described in Figure 1A show that the clones HisACAT1 (the first two lanes) and the (untagged) hACAT1 (third and fourth lanes) stably expressed in CHO cells exhibit an apparent MW of 56 or 50 kDa, respectively, as expected (*19*). In a separate experiment, we monitored the ACAT1 expression levels in CHO cells or in H293 cells by using antibodies against ACAT1 (Figure 1B, top panel) or using antibodies against Flag (Figure 1B, bottom panel). The results show that the HisACAT1/Flag can also be detected by the Flag antibodies as a broad, 56 kDa protein band. On the basis of

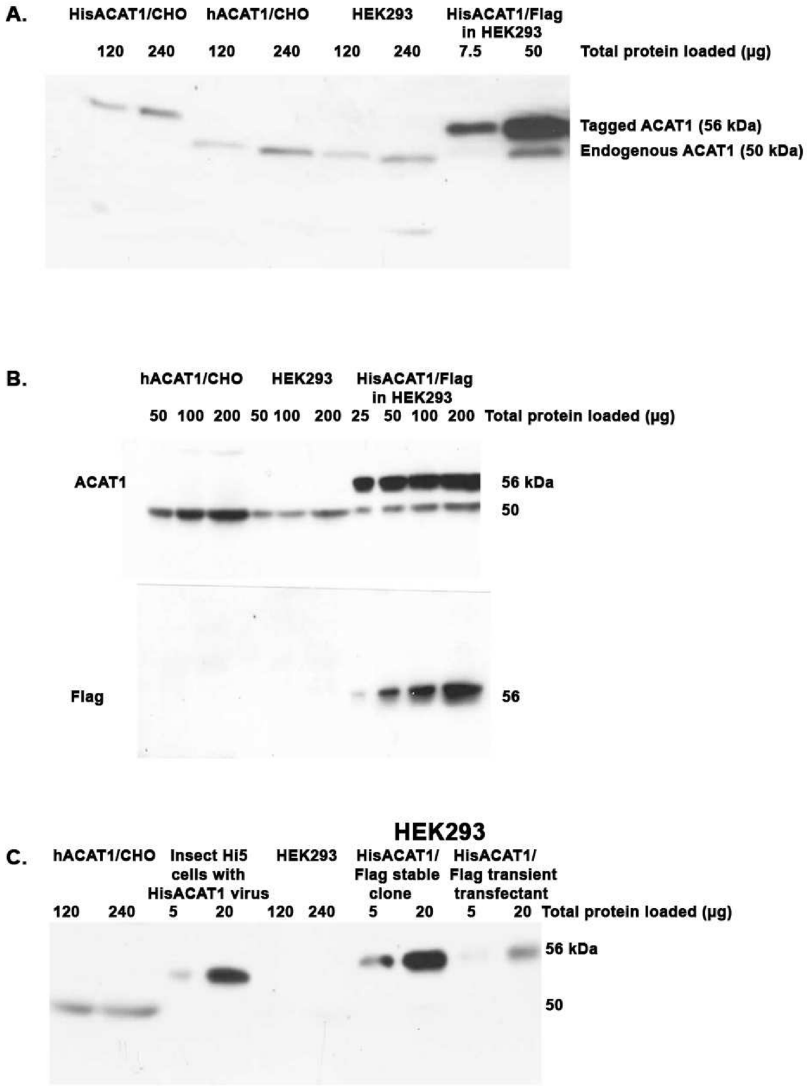

FIGURE 1: Comparison of the tagged (HisACAT1 or HisACAT1/Flag) or the untagged (hACAT1) human ACAT1 protein levels in various expression systems by Western blotting. (A, B) CHO cells vs H293 cells. (C) CHO cells, baculovirus infected insect H5 cells, or H293 cells.

the average of several experiments, we estimate that in H293 cells the HisACAT1/Flag is expressed at protein levels approximately 20 times as high as the endogenous hACAT1. We had previously reported that the relative high protein expression level of HisACAT1 could be achieved by using recombinant baculovirus infection of SF9 cells (*26*) or H5 cells (*27*). Here we performed Western blotting and compared the relative ACAT1 protein expression levels in baculovirus infected H5 cells vs that in the H293 cells stably or transiently expressing the HisACAT1/Flag plasmid. The results (Figure 1C) show that the His ACAT1 expression levels in baculovirus infected H5 cells and the H293 cells stably expressing the HisACAT1/Flag are comparable (lanes 3 and 4 vs lanes 7 and 8). Additional results showed that in H293 cells the HisACAT1/Flag expression level is higher in the stable clone than in the cells that are transiently transfected with the HisACAT1/Flag plasmid (Figure 1C, lanes 7 and 8 vs lanes 9 and 10).

We next compared the ACAT specific enzyme activity expressed in CHO cells vs that in the H293 cells by using cell homogenates solubilized in the detergent CHAPS as the enzyme source. The results (Table 1) show that the enzyme activity of a stable clone of H293 cells expressing HisACAT1/Flag is about 9−10 times higher than that of a stable clone of CHO cells either expressing hACAT1 or expressing HisACAT1. The result also shows that the endogenous ACAT activity in the nontransfected H293 cells is less than 5% that of the stable clone expressing HisACAT1/Flag.

Table 1: [a]

source	ACAT specific activity (pmol min^{-1} mg^{-1})
AC29	0.4
HEK293	37.2
hACAT1 in CHO	131.6
HisACAT1 in CHO	116.5
HisACAT1/Flag in HEK293	1199

[a]The cell extracts were solubilized in 1 M KCl and 2.5% CHAPS and assayed in cholesterol/PC/taurocholate mixed micelles.

Encouraged by the results described above, we used the monolayers of H293 cells stably expressing HisACAT1/Flag as the source to purify the enzyme. The purification procedure (described in detail in Experimental Procedures) is a modification of the procedure previously described (*19*). The major difference occurs at the last purification step. Previously, we had employed

Table 2: Recovery of ACAT Enzyme Activity during Purification[a]

whole cell extract	100%
solubilized enzyme	97
nickel column chromatography	21
Flag column chromatography	32
total recovery	7
total ACAT unit	118 nmol/min
total ACAT1 protein recovered	250 μg

[a]55 of 145 cm^2 dishes of H293 cells stably expressing HisACAT1/Flag were employed as the starting material.

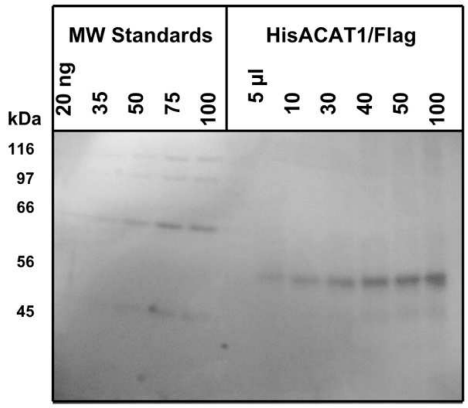

FIGURE 2: Assessment of the purity of HisACAT1/Flag protein by SDS−PAGE and silver staining. Left lanes contained increasing amounts of molecular mass standards (from Sigma); right lanes contained increasing amounts of HisACAT1/Flag at the end of the purification procedure.

the monoclonal antibody against hACAT1 as the affinity probe for column chromatography and eluted the ACAT1 off the column by using a buffer at pH 3−3.5. To avoid using the acidic pH condition which may cause partial enzyme denaturation, we redesigned the recombinant hACAT1 construct by placing the Flag tag at the C-terminus of hACAT1 and employed the monoclonal antibody against Flag as the affinity probe in the second column chromatography step. In this manner, the enzyme could be eluted off the column by using an eluting buffer that contains the Flag peptide at neutral pH. Table 2 summarizes the results of two representative experiments. The total recovery in enzyme units is approximately 7%. The purity of the recombinant hACAT1 is essentially homogeneous, as judged by SDS−PAGE and stained with silver (Figure 2).

Intrinsic Fluorescence of hACAT1. hACAT1 contains 550 amino acids; 15 of them are tryptophan (W) and 29 are tyrosine residues. To avoid the fluorescence contributed by tyrosine, we set the excitation at 295 nm and monitored the emission of fluorescence from 310 to 410 nm. Figure 3A shows the fluorescence emission spectrum of the purified hACAT1 dispersed in 0.5% CHAPS. The spectrum is characterized by a single peak centered at 330 nm, due to tryptophan fluorescence of the protein. We tested the effects of pH on ACAT1 fluorescence; the result showed that the fluorescence intensities of the protein gradually increased when the pH values increased from 6 to 9; however, when the pH value increased from 9 to 10, a 24% decrease in fluorescence intensity occurred (Figure 3A). We noted that quenching of the protein fluorescence signal occurs gradually. When measuring samples at 20 °C in the dark and at various pHs as indicated (from 6 to 10), approximately 10% of the signal is lost in 15 min (Figure 3B), presumably due to photobleaching of the protein fluorescence. We also tested the

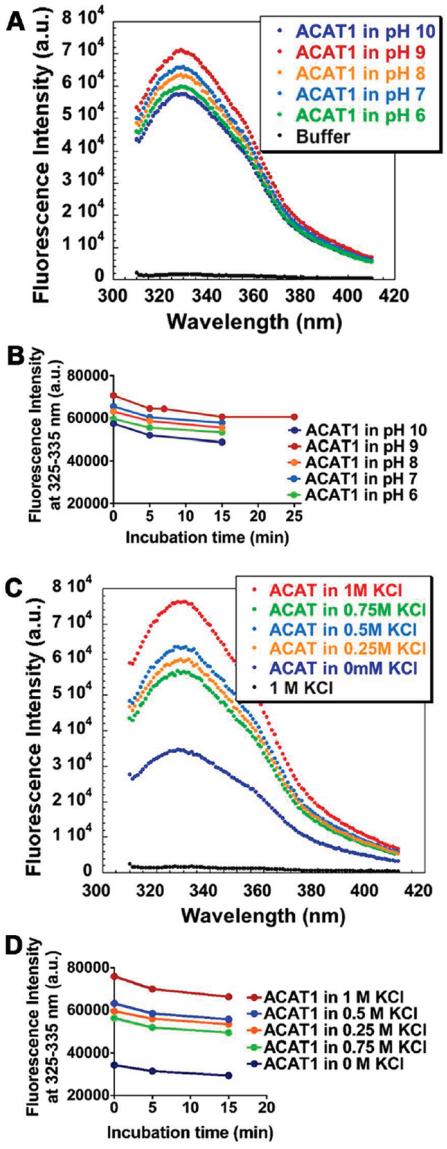

FIGURE 3: Effects of pH and KCl on intrinsic fluorescence of HisACAT1/Flag. (A) The effects of varying pH of buffer from 6 to 10 as indicated. Buffers used: 50 mM citrate for buffer 6; 50 mM phosphate for pH 7 and 8; glycine/NaOH for pH 9 and 10. (B) The stabilities of HisACAT1/Flag fluorescence intensity at various pH conditions. (C) The effects of varying KCl concentrations as indicated. Buffer of pH 7.8 was employed. The background fluorescence of buffers alone (shown at the bottom) is essentially negligible. (D) The stabilities of HisACAT1/Flag fluorescence intensity at various KCl concentrations. The pH was at 7.8.

effect of KCl on ACAT1 fluorescence. The result showed that KCl added at 0.25 M or higher concentrations significantly increased the fluorescence intensities of the protein; at 1 M KCl, the intensity was 2.2-fold higher than the value in the absence of KCl (Figure 3C). This observation correlates well with our previous observation that KCl added at 0.5−1 M concentration increases the enzyme activity of the detergent-solubilized ACAT1 (*19*). Under conditions without or with high KCl, the fluorescence signal gradually decreases, with 8% loss in 5 min and 12% in 15 min (Figure 3D). To minimize the quenching in fluorescence intensity, the fluorescence spectrum of the protein was taken rapidly (within 10−15 s) after the protein was added to the cuvette that already contains the substrate (as described in Experimental Procedures).

Changes in Intrinsic Fluorescence of hACAT1 upon Binding to Fatty Acyl-Coenzyme A or upon Binding to Sterol.

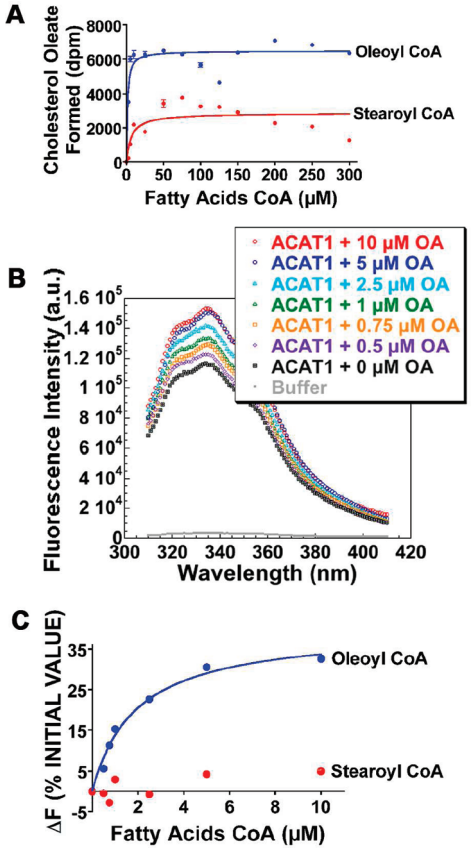

FIGURE 4: Substrate saturation and binding studies of fatty acyl-CoAs with HisACAT1/Flag as the enzyme source. (A) Oleoyl-CoA and stearoyl-CoA substrate saturation curves. Results are representative of two separate experiments. The curves are plotted as hyperbolic. (B) Representative intrinsic fluorescence spectra of hACAT1 in response to increasing concentrations of oleoyl-CoA (abbreviated as OA). (C) Binding curves of oleoyl-CoA and stearoyl-CoA as monitored by changes in intrinsic fluorescence of HisACAT1/Flag. Results are the composite of two separate experiments; the curves are plotted by using the one-site-specific binding program. The Prism software program was used for curve plottings.

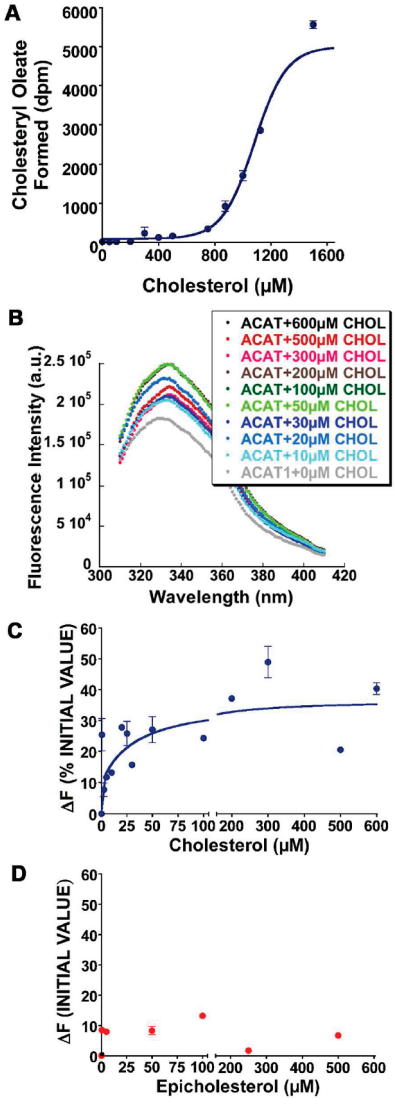

FIGURE 5: Substrate saturation and binding studies of sterols with HisACAT1/Flag as the enzyme source. (A) Cholesterol substrate saturation curve. The cholesterol concentrations varied from 5 to 1600 μM, with oleoyl-CoA concentration kept at 70 μM. The curve is plotted as sigmoidal. (B) Representative intrinsic fluorescence spectra of HisACAT1/Flag in response to increasing concentrations of cholesterol (CHOL). (C) Binding curve of cholesterol as monitored by changes in intrinsic fluorescence of hACAT1; the cholesterol concentrations varied from 0.5 to 600 μM. Results are composite of five separate experiments. The curves are plotted by using the two-site-specific binding program. (D) Binding curve of epicholesterol as monitored by changes in intrinsic fluorescence of HisACAT1/Flag. The epicholesterol concentration varied from 0.5 to 500 μM. Results are the composite of two separate experiments. The curves are plotted by using the one-site-specific binding program. The Prism software program was used for curve plottings.

Prior to conducting binding experiments, we first conducted steady-state enzyme kinetic experiments using purified HisACAT1/Flag as the enzyme source and either oleoyl- (18:1) CoA or stearoyl- (18:0) CoA as the variable substrate, at a constant, saturating level of cholesterol in the CHAPS/PC mixed micelles. The result (Figure 4A) showed that the K_m for oleoyl-CoA is 1.3 μM and is 6.4 μM for stearoyl-CoA; the V_{max} value for oleoyl-CoA is 2.4-fold higher than for stearoyl-CoA. These results confirm and extend previous studies (*28*), demonstrating that ACAT1 prefers oleoyl-CoA to stearoyl-CoA as the substrate. We next conducted binding studies by monitoring the effect of increasing concentrations of oleoyl-CoA on the intrinsic fluorescence of HisACAT1/Flag. The result (Figure 4B) shows that while the peak of the spectrum remained unaltered, the peak height is increased by approximately 32%, with respect to the unliganded ACAT1 protein. A parallel experiment showed that stearoyl-CoA added at increasing concentrations also caused increases in the intrinsic fluorescence of HisACAT1/Flag. However, the maximal change in the peak of the spectrum is much smaller (5% with respect to the unliganded protein). These results (Figure 4C) showed that the oleoyl-CoA-induced fluorescence change is specific and saturable. We analyzed the data in Figure 4C for a simple bimolecular dissociation equilibrium using the Prism program. The results show that the dissociation constant for oleoyl-CoA is 1.9 μM. The changes caused by stearoyl-CoA were too small to derive a reliable dissociation constant.

We had previously conducted steady-state kinetic studies and demonstrated that cholesterol is an efficient substrate as well as an efficient activator, while epicholesterol (which contains the OH moiety at 3α) or enantiomeric cholesterol (which is the mirror image of cholesterol) is neither a substrate nor an activator for ACAT1 (*21*). Here we used the purified HisACAT1/Flag as the enzyme source and conducted cholesterol substrate saturation curve by varying the cholesterol concentration from

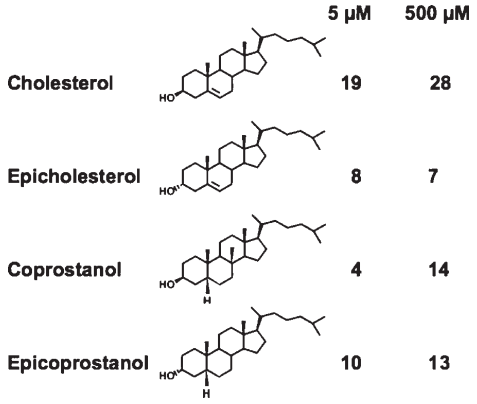

FIGURE 6: Percent changes in intrinsic fluorescence of ACAT by adding various sterols. Experiment was conducted as described in Figure 5C,D. Values were averages of duplicates with deviations less than 10% of the mean.

5 to 1600 μM, with oleoyl-CoA concentration kept at 70 μM. The result showed that the shape of the cholesterol saturation curve is sigmoidal, confirming our previous study when the hACAT1 without the Flag tag was used as the enzyme source (*19*). We next performed the binding experiment by monitoring the effect of increasing concentrations of cholesterol, from 10 to 600 μM, on the intrinsic fluorescence of HisACAT1/Flag. The results (Figure 5B) show that the peak height is positively altered by cholesterol in a concentration-dependent manner, reaching up to 35% with respect to unliganded ACAT1 protein. We estimate that the cholesterol concentration that causes half-maximal spectral change is 35 μM. We conducted a parallel experiment by using epicholesterol as the ligand and showed that epicholesterol at similar concentrations examined (from 0.5 to 500 μM) also caused a positive change in the peak height of the spectrum. However, the maximal changes in the peaks of the spectrum caused by epicholesterol, especially at higher sterol concentrations, are much smaller than those caused by cholesterol. Similar to the result obtained when stearoyl-CoA was tested as the ligand, the changes caused by epicholesterol were too small to derive a reliable binding curve. We next compared the changes in the intrinsic fluorescence of ACAT1 caused by cholesterol, epicholesterol, coprostanol, or epicoprostanol as the ligand. The result (Figure 6) showed that at 5 or 500 μM, the change caused by cholesterol is much larger than the changes caused by either one of the other three sterols.

DISCUSSION

ACAT1 and several of its homologues in the MBOAT family are potential drug targets for treating various diseases, and it is important to carry out structure−function analysis of these enzymes. In the current work, we report the purification of hACAT1 expressed in H293 cells. Based on an average of nine experiments, we obtained 200 ± 40 μg of pure hACAT1 protein with 120 ± 20 nmol/min enzyme units from 55 of 145 cm^2 dishes of H293 cells that stably express HisACAT1/Flag. Previously, we purified hACAT1 from the same number of dishes of CHO cells stably expressing the HisACAT1 to homogeneity with 4.8 nmol/min enzyme units (*19*). The current method thus represents more than 20-fold gain in enzyme units than the previous method. His hACAT1 expressed in baculovirus infected H5 cells could also be purified to homogeneity (*27*). However, the overall recovery of enzyme activity was only approximately 1%; the large loss in activity occurred because the majority of the enzyme activity failed to be bound to the nickel column (results not shown). In both the CHO cell and the H293 cell expression systems, the total yield in enzyme units at the end of the purification procedure is approximately 7%. In the current work, we attached a Flag tag at the C-terminus of hACAT1 and used the Flag peptide dissolved in buffer at neutral pH to elute the ACAT1 off the affinity column; this elution condition is much milder than the one employed previously (*19*).

The expression and purification system reported here provided us with enough pure ACAT1 protein to conduct binding studies between the enzyme and fatty acyl-CoAs by using difference intrinsic fluorescence spectroscopy. The results show that oleoyl-CoA binds to ACAT1 with high affinity. The dissociation constant for oleoyl-CoA is 1.9 μM. The K_d for oleoyl-CoA is similar to its apparent K_m (1.3 μM), suggesting that the enzyme binds to oleoyl-CoA and reaches equilibrium relatively rapidly, while catalysis occurs relatively slowly and constitutes the rate-limiting step. The changes in stearoyl-CoA observed were too small to derive a reliable dissociation constant. The V_{max} for these two substrates differed by 2.4-fold. These results suggest that upon binding to oleoyl-CoA large structural change(s) within the ACAT1 occur(s) to increase the catalytic efficiency of the enzyme.

We also showed that cholesterol caused significant positive changes in the ACAT1 fluorescence spectrum in a concentration-dependent manner. Parallel experiments show that the other three cholesterol analogues, epicholesterol, coprostanol, and epicoprostanol, also elicit positive spectrum changes in ACAT1, but the magnitude of changes induced by either one of these analogues is much smaller than cholesterol. Cholesterol and epicholesterol share the same steroid ring structure and the same isooctyl side chain at ring D but differ at the orientation of the 3-OH moiety at ring A. Coprostanol contains the steroid rings A and ring B in the *trans* configuration (instead of a *cis* configuration as in cholesterol). Epicoprostanol differs from coprostanol at the orientation of the 3-OH moiety at ring A. Cholesterol and epicholesterol interact with membrane phospholipids biophysically and affect membrane properties in very similar manners (*29*, *30*). Coprostanol also interacts with membrane phospholipids but in a manner different from that of cholesterol (*30*). In biological membranes, cholesterol, but not epicholesterol, can directly bind to a variety of membrane proteins in a stereospecific manner to affect their functions (*29*, *31*−*34*). Consistent with this concept, our current results suggest that sterol binding to ACAT1 occurs in two different modes. The first is an indirect one, mediated through its binding to phospholipids, which in turn interacts with the transmembrane domains of ACAT1. The second one involves the direct binding of sterol to certain residues in ACAT1; the direct binding is governed at least in part by the 3β-OH moiety in ring A. The overall change of the ACAT1 fluorescence spectrum caused by cholesterol may be the composite of alteration caused by cholesterol's ability to bind to ACAT1 directly and the alteration caused by cholesterol's ability to interact with phospholipid to affect ACAT1 structural property indirectly. The direct, stereospecific interaction between cholesterol and ACAT1 causes significant structural changes of the enzyme. In the future, simultaneously monitoring the effects of various sterols in altering the physical properties of the micelles vs their effects in altering structural changes of ACAT1 can further test the validity of this interpretation.

ACAT1 contains nine transmembrane domains (TMDs) (*18*). Site-specific mutagenesis and disulfide cross-linking experiments

suggested that several residues (F453, A457, H460, and F479), located within TMD 7 or TMD 8, respectively, played critical roles in maintaining ACAT1 enzyme activity (*35*). In the future, the procedures described here will be employed to test whether any of these residues are involved in binding to cholesterol and/or to oleoyl-CoA. Presently, among the MBOAT enzyme family, ACAT1 is the only one that has been purified to homogeneity. The new information described in our current work may be applicable to study other MBOAT members in general.

ACKNOWLEDGMENT

We thank Dr. Gustav E. Lienhard for careful reading of the manuscript. We thank Dean R. Madden and Larry C. Myers at Dartmouth Medical School and members of the Chang laboratory for helpful discussions during the course of this work. We thank Oneil N. Gardner for participating in the enzyme purification work as an intern of the SURF program.

REFERENCES

1. Chang, C. C., Huh, H. Y., Cadigan, K. M., and Chang, T. Y. (1993) Molecular cloning and functional expression of human acyl-coenzyme A: cholesterol acyltransferase cDNA in mutant Chinese hamster ovary cells. *J. Biol. Chem. 268*, 20747–20755.
2. Cases, S., Novak, S., Zheng, Y. W., Myers, H. M., Lear, S. R., Sande, E., Welch, C. B., Lusis, A. J., Spencer, T. A., Krause, B. R., Erickson, S. K., and Farese, R. V., Jr. (1998) ACAT-2, a second mammalian acyl-CoA:cholesterol acyltransferase. Its cloning, expression, and characterization. *J. Biol. Chem. 273*, 26755–26764.
3. Anderson, R. A., Joyce, C., Davis, M., Reagan, J. W., Clark, M., Shelness, G. S., and Rudel, L. L. (1998) Identification of a form of acyl-CoA:cholesterol acyltransferase specific to liver and intestine in nonhuman primates. *J. Biol. Chem. 273*, 26747–26754.
4. Oelkers, P., Behari, A., Cromley, D., Billheimer, J. T., and Sturley, S. L. (1998) Characterization of two human genes encoding acyl coenzyme A:cholesterol acyltransferase-related enzymes. *J. Biol. Chem. 273*, 26765–26771.
5. Chang, T. Y., Li, B. L., Chang, C. C., and Urano, Y. (2009) Acyl-coenzyme A:cholesterol acyltransferases. *Am. J. Physiol. 297*, E1–E9.
6. Das, A., Davis, M. A., Tomoda, H., Omura, S., and Rudel, L. L. (2008) Identification of the interaction site within acyl-CoA:cholesterol acyltransferase 2 for the isoform-specific inhibitor pyripyropene A. *J. Biol. Chem. 283*, 10453–10460.
7. Ikenoya, M., Yoshinaka, Y., Kobayashi, H., Kawamine, K., Shibuya, K., Sato, F., Sawanobori, K., Watanabe, T., and Miyazaki, A. (2007) A selective ACAT-1 inhibitor, K-604, suppresses fatty streak lesions in fat-fed hamsters without affecting plasma cholesterol levels. *Atherosclerosis 191*, 290–297.
8. Cases, S., Smith, S. J., Zheng, Y. W., Myers, H. M., Lear, S. R., Sande, E., Novak, S., Collins, C., Welch, C. B., Lusis, A. J., Erickson, S. K., and Farese, R. V., Jr. (1998) Identification of a gene encoding an acyl CoA:diacylglycerol acyltransferase, a key enzyme in triacylglycerol synthesis. *Proc. Natl. Acad. Sci. U.S.A. 95*, 13018–13023.
9. Hofmann, K. (2000) A superfamily of membrane-bound O-acyltransferases with implications for Wnt signaling. *Trends Biochem. Sci. 25*, 111–112.
10. Yang, J., Brown, M. S., Liang, G., Grishin, N. V., and Goldstein, J. L. (2008) Identification of the acyltransferase that octanoylates ghrelin, an appetite-stimulating peptide hormone. *Cell 132*, 387–396.
11. Gutierrez, J. A., Solenberg, P. J., Perkins, D. R., Willency, J. A., Knierman, M. D., Jin, Z., Witcher, D. R., Luo, S., Onyia, J. E., and Hale, J. E. (2008) Ghrelin octanoylation mediated by an orphan lipid transferase. *Proc. Natl. Acad. Sci. U.S.A. 105*, 6320–6325.
12. Riekhof, W. R., Wu, J., Jones, J. L., and Voelker, D. R. (2007) Identification and characterization of the major lysophosphatidylethanolamine acyltransferase in *Saccharomyces cerevisiae*. *J. Biol. Chem. 282*, 28344–28352.
13. Shindou, H., and Shimizu, T. (2009) Acyl-CoA:lysophospholipid acyltransferases. *J. Biol. Chem. 284*, 1–5.
14. Chang, C. C. Y., Chen, J., Thomas, M. A., Cheng, D., Del Priore, V. A., Newton, R. S., Pape, M. E., and Chang, T. Y. (1995) Regulation and immunolocalization of acyl-coenzyme A:cholesterol acyltransferase in mammalian cells as studied with specific antibodies. *J. Biol. Chem. 270*, 29532–29540.
15. Sakashita, N., Miyazaki, A., Takeya, M., Horiuchi, S., Chang, C. C. Y., Chang, T. Y., and Takahashi, K. (2000) Localization of human acyl-coenzyme A:cholesterol acyltransferase-1 in macrophages and in various tissues. *Am. J. Pathol. 156*, 227–236.
16. Khelef, N., Soe, T. T., Quehenberger, O., Beatini, N., Tabas, I., and Maxfield, F. R. (2000) Enrichment of acyl coenzyme A:cholesterol O-acyltransferase near trans-golgi network and endocytic recycling compartment. *Arterioscler., Thromb., Vasc. Biol. 20*, 1769–1776.
17. Yu, C., Chen, J., Lin, S., Liu, J., Chang, C. C., and Chang, T. Y. (1999) Human acyl-CoA:cholesterol acyltransferase-1 is a homotetrameric enzyme in intact cells and in vitro. *J. Biol. Chem. 274*, 36139–36145.
18. Guo, Z. Y., Lin, S., Heinen, J. A., Chang, C. C., and Chang, T. Y. (2005) The active site His-460 of human acyl-coenzyme A:cholesterol acyltransferase 1 resides in a hitherto undisclosed transmembrane domain. *J. Biol. Chem. 280*, 37814–37826.
19. Chang, C. C. Y., Lee, C. Y. G., Chang, E. T., Cruz, J. C., Levesque, M. C., and Chang, T. Y. (1998) Recombinant human acyl-CoA: cholesterol acyltransferase 1 (ACAT1) purified to essential homogeneity utilizes cholesterol in mixed micelles or vesicles in a highly cooperative manner. *J. Biol. Chem. 273*, 35132–35141.
20. Zhang, Y., Yu, C., Liu, J., Spencer, T. A., Chang, C. C., and Chang, T. Y. (2003) Cholesterol is superior to 7-ketocholesterol or 7 alpha-hydroxycholesterol as an allosteric activator for acyl-coenzyme A: cholesterol acyltransferase 1. *J. Biol. Chem. 278*, 11642–11647.
21. Liu, J., Chang, C. C., Westover, E. J., Covey, D. F., and Chang, T. Y. (2005) Investigating the allosterism of acyl coenzyme A:cholesterol acyltransferase (ACAT) by using various sterols: in vitro and intact cell studies. *Biochem. J. 391*, 389–397.
22. Bishop, J. E., and Hajra, A. K. (1980) A method for the chemical synthesis of ^{14}C-labeled fatty acylcoenzyme A's of high specific activity. *Anal. Biochem. 106*, 344–350.
23. Reeves, P. J., Kim, J. M., and Khorana, H. G. (2002) Structure and function in rhodopsin: a tetracycline-inducible system in stable mammalian cell lines for high-level expression of opsin mutants. *Proc. Natl. Acad. Sci. U.S.A. 99*, 13413–13418.
24. Ikeuchi, T., Dolios, G., Kim, S. H., Wang, R., and Sisodia, S. S. (2003) Familial Alzheimer disease-linked presenilin 1 variants enhance production of both Abeta 1−40 and Abeta 1−42 peptides that are only partially sensitive to a potent aspartyl protease transition state inhibitor of "gamma-secretase". *J. Biol. Chem. 278*, 7010–7018.
25. Chang, C. C., Lee, C. Y., Chang, E. T., Cruz, J. C., Levesque, M. C., and Chang, T. Y. (1998) Recombinant acyl-CoA:cholesterol acyltransferase-1 (ACAT-1) purified to essential homogeneity utilizes cholesterol in mixed micelles or in vesicles in a highly cooperative manner. *J. Biol. Chem. 273*, 35132–35141.
26. Cheng, D., Chang, C. C., Qu, X., and Chang, T. Y. (1995) Activation of acyl-coenzyme A:cholesterol acyltransferase by cholesterol or by oxysterol in a cell-free system. *J. Biol. Chem. 270*, 685–695.
27. Yu, C., Zhang, Y., Lu, X., Chen, J., Chang, C. C., and Chang, T. Y. (2002) Role of the N-terminal hydrophilic domain of acyl-coenzyme A:cholesterol acyltransferase 1 on the enzyme's quaternary structure and catalytic efficiency. *Biochemistry 41*, 3762–3769.
28. Seo, T., Oelkers, P. M., Giattina, M. R., Worgall, T. S., Sturley, S. L., and Deckelbaum, R. J. (2001) Differential modulation of ACAT1 and ACAT2 transcription and activity by long chain free fatty acids in cultured cells. *Biochemistry 40*, 4756–4762.
29. Gimpl, G., Burger, K., and Fahrenholz, F. (1997) Cholesterol as modulator of receptor function. *Biochemistry 36*, 10959–10974.
30. Xu, X., and London, E. (2000) The effect of sterol structure on membrane lipid domains reveals how cholesterol can induce lipid domain formation. *Biochemistry 39*, 843–849.
31. Romanenko, V. G., Rothblat, G. H., and Levitan, I. (2002) Modulation of endothelial inward-rectifier K^+ current by optical isomers of cholesterol. *Biophys. J. 83*, 3211–3222.
32. Simons, K., and Ikonen, E. (2000) How cells handle cholesterol. *Science 290*, 1721–1726.
33. Westover, E. J., and Covey, D. F. (2004) The enantiomer of cholesterol. *J. Membr. Biol. 202*, 61–72.
34. Gimpl, G. (2010) Cholesterol-protein interaction: methods and cholesterol reporter molecules. *Subcell. Biochem. 51*, 1–45.
35. Guo, Z. Y., Chang, C. C., and Chang, T. Y. (2007) Functionality of the seventh and eighth transmembrane domains of acyl-coenzyme A: cholesterol acyltransferase 1. *Biochemistry 46*, 10063–10071.